NeuroImage 243 (2021) 118512

Contents lists available at ScienceDirect

NeuroImage

journal homepage: www.elsevier.com/locate/neuroimage

Neuronal biomarkers of Parkinson's disease are present in healthy aging

Juanli Zhang [a,b,*], Mina Jamshidi Idaji [a,c,d], Arno Villringer [a,e], Vadim V. Nikulin [a,f,g,*]

[a] Department of Neurology, Max Planck Institute for Human Cognitive and Brain Sciences, Leipzig, Germany
[b] Department of Neurology, Charité – Universitätsmedizin Berlin, Berlin, Germany
[c] Machine Learning Group, Technical University of Berlin, Berlin, Germany
[d] International Max Planck Research School NeuroCom, Leipzig, Germany
[e] Department of Cognitive Neurology, University Hospital Leipzig, Leipzig, Germany
[f] Centre for Cognition and Decision Making, Institute for Cognitive Neuroscience, National Research University Higher School of Economics, Moscow, Russian Federation
[g] Neurophysics Group, Department of Neurology, Charité – Universitätsmedizin Berlin, Berlin, Germany

ARTICLE INFO

Keywords:
Resting state EEG
Healthy aging
Parkinson's disease
PAC
Beta burst

ABSTRACT

The prevalence of Parkinson's disease (PD) increases with aging and both processes share similar cellular mechanisms and alterations in the dopaminergic system. Yet it remains to be investigated whether aging can also demonstrate electrophysiological neuronal signatures typically associated with PD. Previous work has shown that phase-amplitude coupling (PAC) between the phase of beta oscillations and the amplitude of gamma oscillations as well as beta bursts features can serve as electrophysiological biomarkers for PD. Here we hypothesize that these metrics are also present in apparently healthy elderly subjects. Using resting state multichannel EEG measurements, we show that PAC between beta oscillation and broadband gamma activity (50–150 Hz) is elevated in a group of elderly (59–77 years) compared to young volunteers (20–35 years) without PD. Importantly, the increase of PAC is statistically significant even after ruling out confounds relating to changes in spectral power and non-sinusoidal shape of beta oscillation. Moreover, a trend for a higher percentage of longer beta bursts (> 0.2 s) along with the increase in their incidence rate is also observed for elderly subjects. Using inverse modeling, we further show that elevated PAC and longer beta bursts are most pronounced in the sensorimotor areas. Moreover, we show that PAC and longer beta bursts might reflect distinct mechanisms, since their spatial patterns only partially overlap and the correlation between them is weak. Taken together, our findings provide novel evidence that electrophysiological biomarkers of PD may already occur in apparently healthy elderly subjects. We hypothesize that PAC and beta bursts characteristics in aging might reflect a pre-clinical state of PD and suggest their predictive value to be tested in prospective longitudinal studies.

1. Introduction

Aging is associated with alterations in metabolism, neurotransmission, hormonal and immune dysregulation, and inflammation; thus leading to diverse neurocognitive impairments (Kim et al., 2017; Sibille, 2013; Zhuang et al., 2018). Healthy aging is accompanied by the loss of dopaminergic (DA) neurons (Rudow et al., 2008), and it is assumed that the clinical signs of Parkinson's disease in humans appear when the DA in the substantia nigra pars compacta (SNc) are degenerated by up to 60%–70% (Cheng et al., 2010; Darden, 2007). Although elderly people often demonstrate mild parkinsonian signs including rigidity, bradykinesia, tremor and problems with gait balance (Louis and Bennett, 2007), these signs do not meet the established clinical criteria for Parkinson's disease (PD) (Marsili et al., 2018). Yet, aging is the single most significant factor influencing the clinical presence and progression of PD (Hindle, 2010). A close association between aging and PD is further supported by the findings in non-human primates demonstrating that both processes have multiple similar biological features and share the directionality of alterations in the nigrostriatal DA system. This in turn leads to a hypothesis that aging is associated with biological changes (particularly in dopamine system) creating vulnerable conditions potentially serving as a foundation for PD (Collier et al., 2017).

Given a close relationship between PD and aging, it is tempting to speculate that this relation can also be reflected in electrophysiological brain signals. Interestingly, using invasive and non-invasive electrophysiological methods, several signatures of PD have been identified. But, to the best of our knowledge, it is not known whether similar changes are also present in apparently healthy elderly subjects compared to the young ones. The most pronounced electrophysiological signature of PD is represented by abnormally elevated beta oscillatory activity in the subthalamic nucleus (STN) (Alexandre Eusebio and Brown, 2009;

* Corresponding authors.
E-mail address: juanlizhang@cbs.mpg.de (J. Zhang).

https://doi.org/10.1016/j.neuroimage.2021.118512.
Received 10 August 2021; Accepted 23 August 2021
Available online 26 August 2021.

Brittain et al., 2014; Brown, 2003; Crowell et al., 2012; De Hemptinne et al., 2015; Hammond et al., 2007; Kühn et al., 2009; Little and Brown, 2014; Oswal et al., 2013; Weinberger et al., 2006). Beta power in the STN is correlated with bradykinesia (A. Eusebio et al., 2011; Chen et al., 2010; R. Levy et al., 2002) and is attenuated by levodopa (Kühn et al., 2009; Weinberger et al., 2006) and by deep brain stimulation (DBS) (Müller and Robinson, 2018; Ray et al., 2008; Wingeier et al., 2006). Moreover, a higher incidence of longer beta bursts in the STN has been shown to correlate positively with clinical impairment (Tinkhauser et al., 2017a, 2017b). At the level of the cortex, however, divergent studies demonstrated that either a decrease (Stoffers et al., 2007; Whitmer et al., 2012) or an increase (Melgari et al., 2014) in cortical beta power can occur during successful symptomatic therapy of PD. Notably, an alternative cortical biomarkers for PD is phase-amplitude coupling (PAC) between the phase of beta oscillations and the amplitude of broadband activity (also referred to here as "broadband gamma") extending from 50 to 200 Hz (De Hemptinne et al., 2013, 2015). Increased cortical PAC observed in PD patients reflects a rather stereotypical neuronal recruitment pattern of sensorimotor areas and is hypothesized to promote rigidity and akinesia—cardinal symptoms of PD. Moreover, cortical beta-gamma PAC is considerably decreased during clinically effective DBS in the STN and by levodopa treatment (De Hemptinne et al., 2013; Swann et al., 2015). Non-invasive scalp-EEG analyses of cortical beta-gamma PAC (A. M. Miller et al., 2019; Swann et al., 2015) confirmed that PAC is indeed stronger in PD patients compared to age-matched healthy subjects. With respect to beta burst dynamics, a study by Tinkhauser et al. (2018) showed that longer beta bursts in the cortex coincide with longer burst in the STN showing further that episodes of elevated beta occur simultaneously in the basal ganglia and cortex thus limiting information coding capacity and leading to deterioration of movement performance. And more recently, a study using ECoG in M1 demonstrated a higher percentage of longer beta bursts in PD patients compared to the subjects without PD (O'Keeffe et al., 2020). Taken together, these cortical features, namely PAC and beta burst dynamics, have been consistently reported in PD. Whether the two PD biomarkers are related to each other, so far, has been studied only in very few studies which suggested a close relationship between the two (Meidahl et al., 2019; O'Keeffe et al., 2020). However, none of them investigated their relationship in a topographical manner. Yet, a different topographical pattern may indicate distinct underlined pathophysiology. Thus, investigating the presence and relationship of such biomarkers using multichannel EEG might aid to better understanding the associated neurophysiological processes in PD and healthy aging.

Given the above-mentioned association between aging and PD, in the present study, we tested the hypothesis that electrophysiological signatures of PD at the cortical level, that is, PAC between the phase of beta oscillations and the amplitude of broadband gamma activity, as well as the incidence of longer beta bursts, is more pronounced in elderly compared to young subjects. Moreover, we expected that this effect would be most prominent in the sensorimotor areas of the cortex. We tested these hypotheses using the recently acquired LEMON dataset (Babayan et al., 2019) containing a large number of healthy young and old subjects with multichannel EEG.

2. Materials and methods

2.1. Subjects and task

The recruitment of the participants was carried out in two steps. First, participants were pre-screened by telephone with a semi-structured interview. Before the study, further individual screening was performed by a study physician who assessed for exclusion criteria such as diagnosis of hypertension, cardiovascular disease, history of neurological disorder or psychiatric disease, history of malignant disease etc. (Babayan et al., 2019). Participants were instructed to sit calmly and comfortably in a chair and the recording was conducted in a sound-shielded room. The sessions consisted of 16 segments each lasting 60 s with each such segment related to interleaved eyes-closed (EC) or eyes-open (EO) condition. Therefore, each condition (EC or EO) lasted 8 min. In this study, only the data during eyes closed periods were included for further analysis. We included all the elderly subjects and selected an equally sized group of gender-matched young subjects. In total, there were 137 subjects: 71 young (age 20–35 years, mean age = 25.61, SD = 3.17, 24 females) and 66 old (age 59–77 years, mean age = 67.35, SD = 4.81, 31 females).

The Alertness subtest of the Test of Attentional Performance (TAP; orig. "Testbatterie zur Aufmerksamkeitsprüfung"; version 2.3; Zimmermann & Fimm, 2012) measures alertness and reaction speed. During this test, a cross appears on a screen at randomly varying intervals to which the subject should respond as quickly as possible by pressing a key. The mean reaction time over the trials is derived as a measure of intrinsic alertness for each subject, i.e. higher reaction time scores indicate a lower performance.

2.2. EEG recordings

62-channel EEG was acquired with BrainAmp MR-plus amplifiers using ActiCAP electrodes (both Brain Products, Germany). Electrode montage was based on the international standard 10–20 system with FCz being the reference during recording. Electrode impedance was kept below 5kΩ. Recordings were digitized at a sampling frequency of 2500 Hz and bandpass filtered between 0.015 Hz and 1 kHz.

2.3. Data analysis

2.3.1. Data pre-processing

In order to keep our data pre-processing comparable to previous EEG PD studies, we implemented it in an analogous manner to A. M. Miller et al. (2019) and Jackson et al. (2019). EEG data were analyzed with Matlab (The MathWorks Inc, Natick, Massachusetts, USA) using custom scripts and EEGLab toolbox (version 14.1.2; (Delorme and Makeig, 2004)) functions. At the first step, the data were down sampled to 512 Hz. A highpass filter at 1 Hz was then applied to remove low frequency drifts (two-way FIR filter, order = 1536, eegfilt.m from EEGLab). The continuous EEG data were then segmented into EC and EO conditions. Subsequently, independent component analysis (ICA – Infomax algorithm implemented in EEGLab) was used to remove physiological and non-physiological artifacts including cardiographic component, eye movements and blinks, muscle activity and line noise in the EC data. Next, the data were re-referenced to a common average. In the last stage, data were still examined visually for the presence of residual artifacts and segments contaminated by these events were marked and then excluded from the analysis. There was no difference between the groups in the length of the data (on average 444.36 s for elderly and 455.22 s for younger groups, respectively) included for further analysis (Wilcoxon rank sum test, $p = 0.2015$).

2.3.2. Spectral analysis

Power spectral density (PSD) was calculated using '*pwelch'* function in MATLAB, with a Hamming window of 512 samples and a 50% overlap. The average PSD for beta band was obtained by averaging the spectral density in the beta frequency range (13–30 Hz). Individual beta peaks were detected using '*findpeaks*' function in the frequency range 13–30 Hz.

2.3.3. Phase amplitude coupling (PAC)

PAC was calculated using the Kullback-Leibler-based modulation index method (Tort et al., 2008). Briefly, the modulation index (MI) quantifies the degree of deviation of the phase-modulated amplitude from the uniform distribution. The distribution of the normalized instantaneous amplitude envelope was computed for 18 phase bins, each covering 20 radians. A comparison of this distribution to the uniform distribution

was quantified with the Kullback-Leibler distance measure. The computed MI value is between 0 and 1 (0 for no coupling, and 1 for when the phase of the slower oscillation and the amplitude of the faster oscillation is fully coupled). MIs were calculated for phase-providing frequency across the 4–50 Hz range using a sliding window with a step size of 2 Hz and a bandwidth of 2 Hz, whilst the range for the amplitude-providing frequency varied from 4 to 170 Hz with a step size of 4 Hz. Since PAC measures require the filter for the amplitude extraction from faster frequency activity to have a bandwidth at least as great as the range of slower frequencies of interest, at each amplitude-providing frequency, we used a filter with a bandwidth as wide as that of the center-frequency of the phase-providing oscillation. The phase of the lower frequency and the amplitude of the higher frequency components were obtained using Hilbert transform after bandpass filtering using a two-way finite impulse response filter (FIR) (eegfilt.m with '*fir1*' parameters from EEGLab, with the order of three cycles of lower cutoff frequency). To obtain meaningful values, we started the calculation between frequency pairs in which amplitude-providing frequency was always higher than the phase-providing one. The MIs across all the possible frequency pairs can be displayed as a phase-amplitude comodulogram.

A PAC value was derived for each channel and each subject as the mean of the MI values over the beta range (13–30 Hz) for phase-providing frequency and broadband gamma frequency range (50–150 Hz) for the amplitude-providing frequency. This approach has also been used in previous studies (A. M. Miller et al., 2019; Swann et al., 2015).

2.3.4. Non-sinusoidal waveform shape measure

In order to rule out the possibility that the statistical PAC could be due to the sharp edges of the waveforms (Kramer et al., 2008), non-sinusoidality of beta oscillation was quantified using sharpness and steepness ratios. The method proposed by (Cole et al., 2017) was used for this purpose. Below we elaborate on these calculations.

2.3.4.1. Sharpness ratio. First, we bandpass filtered (13–30 Hz, eegfilt.m from EEGLab, order = 118) the raw time series to obtain beta oscillations, for which we then identified rising and falling zero-crossing points. Then, in the raw signal, indices of maximum and minimum voltages between zero-crossings were found as the locations of peaks and troughs. Peak (trough) sharpness was defined as the mean voltage difference between the peak (trough) and neighboring three time points, which are ~6 ms before and after the peak (trough) (Cole et al., 2017). Finally, the sharpness ratio was calculated as the absolute value of the log-transform of the ratio of peak sharpness to trough sharpness.

2.3.4.2. Steepness ratio. The rise steepness was defined as the largest voltage rise between two subsequent data points (first derivative) in the time period between a trough and the peak after it. In the same manner, the decay steepness was calculated as the largest voltage drop between a peak and the trough following it. Similarly, steepness ratio was calculated as the absolute value of the log-transform of the ratio of rise steepness to decay steepness.

2.3.5. Beta bursts definition and characteristics

We referred to the methods proposed by Tinkhauser et al. (2017a) and Tinkhauser et al. (2017b) to estimate beta burst dynamics. First, we identified the mean beta peak frequency for each individual by averaging the peak frequencies over the channels. Then we detected the beta bursts in a frequency range of ± 5 Hz around the individual beta peak frequency (~15–25 Hz). Raw signal was bandpass filtered, and the amplitude envelope of the filtered data was extracted using Hilbert transform. A beta burst was defined as the time interval where the amplitude exceeds a certain threshold and stays above threshold for more than 100 ms (at least two cycles). We explored the region-specific differences of bursts characteristics with the threshold fixed at the 65th percentile of the amplitude. Moreover, to investigate the impact of the burst thresholds, we included the analysis for a wide range of thresholds (percentiles 50, 55, 60, 65, 70, 75, 80, 85, and 90).

The histogram of the burst duration for each channel was investigated by binning the duration of the beta bursts into nine windows, namely 0.1–0.2 s, 0.2–0.3 s, 0.3–0.4 s, 0.4–0.5 s, 0.5–0.6 s, 0.6–0.7 s, 0.7–0.8 s, 0.8–0.9 s, and >0.9 s. Since total burst duration varies across channels and subjects, the histogram was normalized by the total number of beta bursts. Another feature of bursts, that is, incidence rate, was defined as the number of bursts per time unit (bursts/(second)). For the analysis across different threshold percentiles, we focused on two key features, namely mean burst duration and mean burst amplitude across all beta bursts.

2.3.6. Source space analysis

For the localization of neuronal sources we applied inverse modeling to project the EEG sensor recordings to cortical source level. After the EEG was preprocessed, EEG sensor signals were bandpass filtered within the frequency range of interest (eegfilt.m from EEGLab). We used the eLORETA algorithm (exact low resolution brain electromagnetic tomography, as implemented in the M/EEG Toolbox of Hamburg (METH, https://www.nitrc.org/projects/meth/) (Haufe and Ewald, 2016)) for inverse modeling and the New York head model with approximately 2000 vertices (Huang et al., 2016) to acquire the leadfield matrix. The cortical vertices were grouped into 96 regions of interest (ROIs) based on Harvard-Oxford atlas (Desikan et al., 2006). The time series estimated for each vertex was used for further analysis.

Specifically, for the PAC and beta band power analysis, we first estimated the metrics based on the time series from each vertex. Subsequently, we averaged the values across all the vertices within each ROI. To calculate PAC in a uniform way, we obtained the source reconstructed signal from beta band (13–30 Hz) and broadband gamma (50–150 Hz) to estimate the phase for lower frequency and amplitude for higher frequency components for each vertex, respectively. Then MI values were estimated for each vertex and further for each ROI from each subject. Beta power values were computed analogously by averaging PSD values over beta frequency range (13–30 Hz) for each vertex. Then, the ROI-based power value was estimated by averaging over the vertices within each ROI.

With respect to beta burst dynamics, we bandpass filtered data using the approach presented above for the sensor level (see Section 2.3.5.) and then projected the bandpass filtered sensor data to the cortical sources. Afterwards, singular value decomposition (SVD) was applied to the signals within each ROI in order to extract a representative ROI-based signal. Using SVD of the time series of all vertices within each ROI, the dominant time course of each ROI was extracted by preserving the first dominant SVD component. Thus, the 61-channel sensor level signal was transformed to 96-ROI signal at source level. Further analysis remained the same as for the sensor level.

2.3.7. Statistical tests

Statistical comparisons across groups were performed using a non-parametric Wilcoxon rank sum test between the old and young groups. To correct for multiple comparisons, false discovery rate (FDR) method was used according to Benjamini and Hochberg (1995) when multiple electrodes in sensor space, ROIs in source space, frequency bins and burst window bins were compared.

For the MI-comodulogram comparison between two groups at a single channel (C3), we performed frequency-frequency space cluster-based permutation procedure by using the 'Monte Carlo' method, as implemented in FieldTrip (Oostenveld et al., 2011). In brief, with 2000 permutations across the randomly shuffled labels for old and young groups, one can create the distribution of cluster statistics under the null hypothesis that there is no significant cluster. For each randomization, cluster level statistics (taking the sum of t values of all the frequency pair points within each cluster) were computed and the largest cluster statistic was

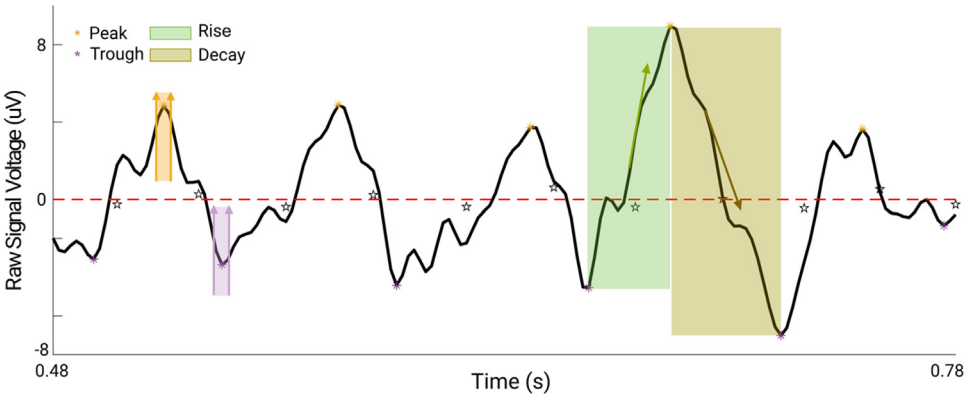

Fig. 1. Schematic illustration of the waveform shape estimation. Peaks and troughs in the raw signal that lie between the adjacent zero crossings identified from filtered beta band signal are color coded *: orange for peaks and purple for troughs. The light green area marks the rise period between a trough and subsequent peak to determine the rise steepness. Dark green area indicates the decay area where the decay steepness was estimated.

entered into the null distribution. Finally, the observed cluster in the empirical data was compared against the null distribution, and a p value below 0.05 (two tailed) was considered significant.

A correlation between different measures was performed using Spearman' approach. For the topographical correlation pattern, correlation strength was calculated for each channel or each ROI across the subjects, and then FDR was applied to correct for multiple comparisons across the channel/source space. The final correlation pattern was displayed as a head topography or on a standard reconstructed cortical surface model.

3. Results

3.1. PAC between beta band and broadband gamma activity is elevated with aging

3.1.1. PAC is elevated in sensorimotor areas in the elderly

To test the hypothesis that in the sensorimotor areas of the cortex PAC is elevated in the elderly, we first analyzed MI values from one of the electrodes typically attributed to the sensorimotor cortex (C3) (Swann et al., 2015). Fig. 2A shows mean comodulograms of MI at electrode C3 for each group. A prominent coupling can be observed between the phase of beta to low gamma and the amplitude of 50–150 Hz frequency range in the elderly (left panel) compared to the young group (right panel). Using cluster analysis, we examined the MI comodulograms for significant differences between the two groups. Fig. 2B shows a significant beta-gamma coupling group difference at electrode C3. The outlined cluster indicates a significant difference of PAC between the beta phase (13–30 Hz) and broadband gamma (50–150 Hz) frequency range, as well as PAC between low gamma phase frequency (30–50 Hz) and broadband gamma amplitude frequency. Further, we investigated at which phase providing frequencies the average PAC between the gamma amplitude and the phase from examined frequency differs between the two groups. This was done by computing PAC for the amplitude from 50 to 150 Hz for each phase-providing frequency window from 4 to 50 Hz (2 Hz width). The panel C of Fig. 2 depicts a significant PAC difference profile occurring starting from around 12 Hz extending up to low gamma range($^*p < 0.05$, after FDR). Boxplots for PAC values from MIs averaged over 13–30 Hz for beta phase and 50–150 Hz for broadband gamma amplitude are presented in Fig. 2D. Although there was a considerable overlap between PAC values in two groups, the statistical analysis confirmed that the elderly group was characterized by significantly elevated PAC between beta oscillation and broadband gamma activity ($^*p = 0.0147$). Finally, we used normalized amplitude of broadband gamma (50–150 Hz) sorted according to the phase bins from beta band (see Section 2.3.3.) in order to see how it is modulated by the phase of beta oscillations (13–30 Hz). The upper panel E in Fig. 2 shows the mean of the normalized amplitude distribution at C3 in each group. Generally, broadband gamma amplitude is largely coupled to non-peak phase of the beta oscillations by showing a strongest amplitude after (not at) $\pi/2$ radian in both groups. In addition, one can see elderly subjects showed a higher degree of modulation compared to young subjects. Circular bar plot in the bottom further confirms there is a certain age-dependent phase specificity: beta phase predominantly distributed within pi/6 ~ 2*pi/3 when the highest amplitude occurred for both age groups.

Although we have found that the amplitude from broadband gamma range is coupled to the phase of beta and low gamma bands, further tests revealed that low-gamma phase driven PAC could be, to a very large extent, accounted for by simultaneous phase-phase coupling. This in turn indicates that low-gamma modulated PAC is likely to be driven by the sharpness of the low-gamma band waveform which is probably due to residuals of muscle activity (see supplemental analysis 1.1.). These results further justified our focus on beta-gamma PAC, which has previously been shown to be exaggerated in PD (de Hemptinne et al., 2013; Swann et al., 2015; Jackson et al., 2019; A. M. Miller et al., 2019).

3.1.2. PAC difference topography in aging demonstrates a left-hemisphere dominant pattern

To investigate the spatial pattern of PAC difference, we calculated the PAC values across all channels and performed comparisons (Wilcoxon rank sum test) between the two age groups using FDR-correction. Fig. 3A depicts the scalp topography of the difference between the two age groups. The comparison was conducted for the PAC values which were derived by averaging MI values over the beta range (13–30 Hz) for phase frequency and broadband gamma range (50–150 Hz) for amplitude frequency. Electrode labels are present only for the significant differences ($p < 0.05$, FDR corrected). The pattern has left-hemisphere dominant distribution over the centro-temporal areas and also extends to frontal areas. Moreover, we demonstrated the statistical PAC values using surrogate procedure are significant over sensorimotor areas within each group and the difference pattern based on the statistical PAC value are well overlapping with Fig. 3A obtained from raw PAC values (see details in Figure S7 in the supplemental material). At source space, we calculated the PAC value for each ROI and each subject (see Section 2.3.6.) and performed the comparison (Wilcoxon rank sum test) between groups (old vs. young) for all ROIs. Fig. 3B shows that PAC values are significantly increased in the elderly group. This result confirms the pattern which demonstrates left hemisphere dominance in PAC differences, with the most profound difference being localized in the left pre- and post-central gyri (extending to superior frontal and supramarginal gyri). Additionally, to rule out possible confounders which might contribute to age-related statistical PAC differences, we performed additional analyses on the power and non-sinusoidal waveform shape of beta oscillations (see supplemental analyses 1 and 2). These analyses confirmed further that the beta phase driven PAC difference between the two age groups is not likely to be driven by either beta band power or non-sinusoidality of beta waveform, although waveform

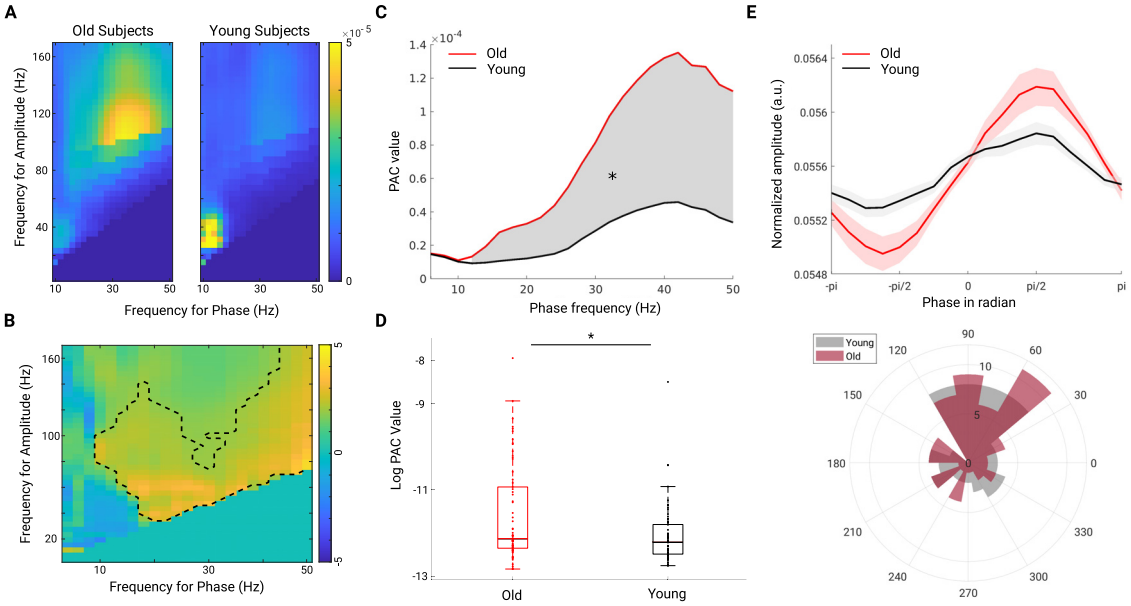

Fig. 2. PAC between beta, low-gamma band oscillations and broadband gamma activity is increased in the old compared to the young group at electrode C3. A. Mean comodulograms of modulation index across subjects in each group. Color bar indicates the PAC strength. B. The dashed black line shows the identified significant MI cluster of the difference-comodulogram (cluster-based permutation test, $p = 0.01$). Color bar represents the statistical value. C. Red and black lines show the mean of MI values across old and young subjects, respectively, within each phase-frequency window (estimated from broadband gamma amplitude frequency range (50–150 Hz)). Gray shaded areas show the phase frequencies which are coupled significantly stronger to the broadband gamma activity in elderly compared to young subjects. This is after FDR correction for multiple comparisons (across all the analyzed phase frequencies, $^*p < 0.05$). D. Boxplots of the averaged MI values over 13–30 Hz for beta phase and 50–150 Hz for broadband gamma amplitude for each age group. There is a significant difference between old and young groups (old vs. young) (two tailed Wilcoxon rank sum test, $^*p = 0.0147$) although one can also observe a considerable overlap between PAC values belonging to both groups. E. The upper panel shows the mean of the normalized broadband gamma amplitude according to the beta phase (from $-\pi$ to π). Red and black lines represent the mean of the normalized amplitude for the elderly and young group, respectively. Shaded areas indicate the standard error of the mean (SEM) across subjects within a group. Circular bar plot in the bottom shows the distribution of preferred beta phase at which the maximal coupling occurred across the subjects within the elderly (in red) and the young group (in gray). Beta phase predominantly distributed within pi/6 ~ 2*pi/3 when the highest amplitude occurred for both age groups.

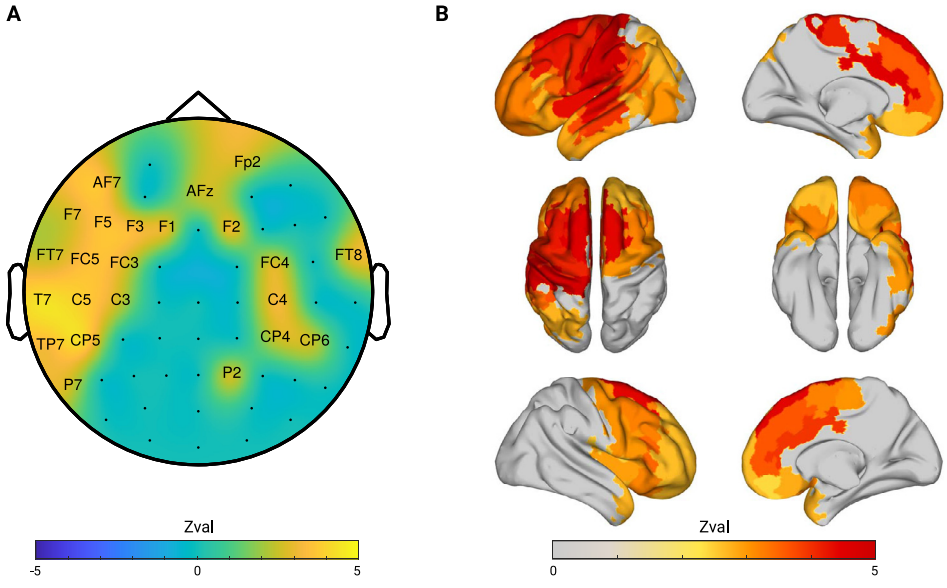

Fig. 3. Spatial topography of PAC difference between the two age groups (old vs. young). PAC values were calculated by averaging over beta range (13–30 Hz) for phase frequency and broadband gamma (50–150 Hz) range for amplitude frequency. A. Statistical comparisons (Wilcoxon rank sum test) were performed between the two age groups (old vs. young). The electrodes with labels show significant differences after FDR correction across all channels. B. Spatial difference pattern of PAC calculated in source space between the two age groups after FDR correction across ROIs. The topography demonstrated that the most significant difference occurred in the left precentral gyrus. Color bar indicates the test statistic. Positive values indicate stronger PAC values in the elderly group.

of the oscillation could represent another neural signatures characterizing aging (see supplemental discussion 1.).

3.1.3. Behavioral relevance of PAC shows differential pattern within two age groups

PAC has been shown to be associated closely to the severity of movement dysfunction in patients with PD. We were also interested to test how PAC could relate to movement performance. However, in this open dataset, movement task was not specifically designed. Yet, to a certain degree a motor readiness can be assessed with the TAP-alertness task. This task measures cognitive alertness (alertness of Test of Attentional Performance, Zimmermann et al., 2012) which is an objective marker of the ability to maintain an alert state of response readiness, and it has been shown to decline with age (McAvinue et al., 2012). Here, the

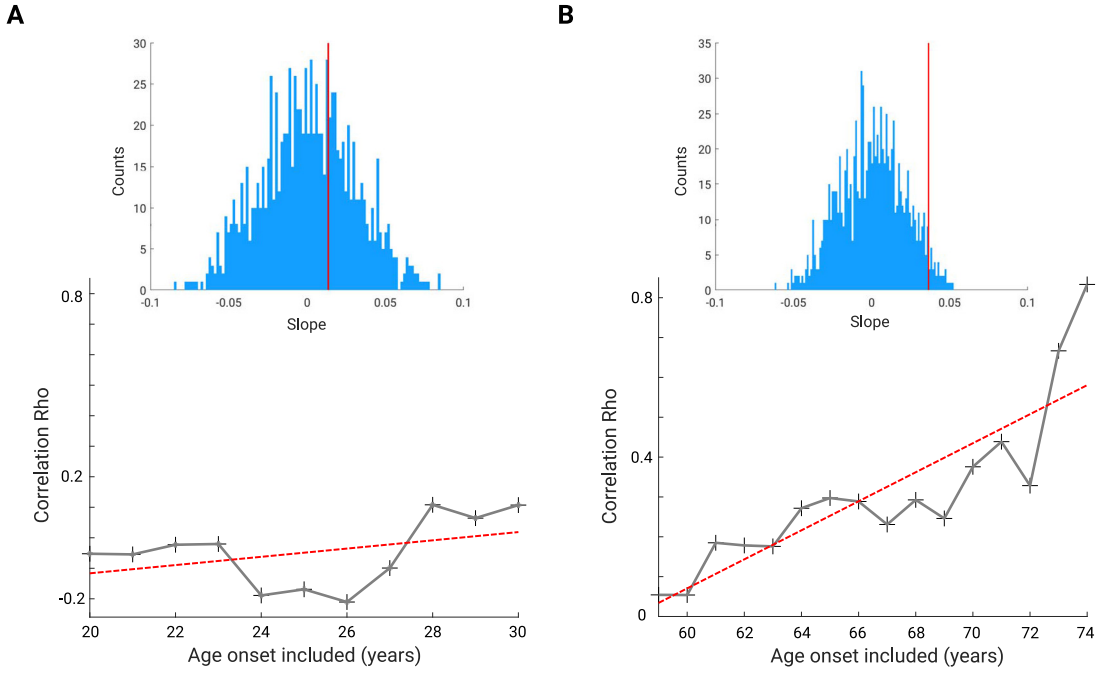

Fig. 4. Correlation between PAC and reaction time in subgroups with increasing age onset. A. Correlation between PAC and TAP-alertness reaction time in young group. X axis represents the age onset for which the subjects were included from for the subgroup. For instance, for the young subjects with age older than 26 (but still younger than 35), there is a negative but non-significant correlation between PAC and reaction time (Rho = −0.2106, p = 0.2320). The red dashed line shows the regression line for the correlation coefficients. The histogram shows the distribution of the slopes from permuted data (1000 times) while the vertical red line indicates the value where the observed actual slope (slope = 0.0135, p = 0.3260) is situated. B. The same analysis for the elderly group. There is a tendency for increasing correlation strengths with the age from which the subgroup starts. The red dashed line shows the regression line for the correlation coefficients within each subgroup while including older subjects from 59 years to 74 years old. The histogram shows the distribution of the slopes from randomized data (1000 times) while the vertical red line indicates where the regression slope obtained by the unpermuted data (slope = 0.0364, p = 0.0320) stands. P value is thus a fraction of slopes which are larger than the value corresponding to the red line.

mean reaction time for each subject was utilized to quantify the alertness where lower scores indicate better performance. To obtain a reliable measure of PAC from the sensorimotor areas for each subject, we took the mean of PAC values from left and right precentral gyri. First, we performed correlation analysis between PAC and the reaction time within each age group, and no significant results were observed either in the elderly group (Rho = 0.0542, p = 0.6654), or in the young group (Rho = −0.0524, p = 0.6645). We hypothesized that this might be due to the fact that the included elderly subjects were generally rather healthy (due to very strict exclusion criteria) and if we narrow down the aging group, the relationship probably would be more obvious. To test this hypothesis, we performed correlation analyses on the subgroups in which the inclusion criteria of age onset were increased stepwise, both for elderly and younger groups. In Fig. 4A, the strengths of correlations with increasing age onsets from 20 to 30 years in the young group are shown; all the correlations were not significant (sample size >= 7). Fig. 4B demonstrates the results of the same analysis for the elderly group (59 to 74 years old, sample size >= 8). We observed a trend for increased correlation strengths with increasing age.

To rule out the possibility that the observed tendency may result from a sub-sampling procedure itself (with age onset increasing, less samples are available), we further performed a permutation procedure to test the significance of the trend in correlation between PAC and reaction time in elderly participants. In brief, we randomized the elderly subjects and then performed all the steps as described above for the experimental data. Then, a linear regression line was fitted to the correlation coefficients and the slope of a linear regression was taken to build the null distribution. In total, the randomization was performed 1000 times, and a final p value was obtained for the observed regression slope compared to the null distribution obtained by permutations. As shown in the histograms of Fig. 4, the vertical red lines indicate the value of the regression line for the younger group (slope = 0.0135, p = 0.3260) and the older group (slope = 0.0364, p = 0.0320), respectively. This demonstrates that the observed tendency to increase the positive association between PAC and reaction time occurred only for the group of elderly subjects while we controlled for the possible biasing effects associated with the sub-sampling procedure.

3.2. Properties of beta bursts are altered with aging

3.2.1. Aging is accompanied by a higher percentage of long burst events

Fig. 5A illustrates the change of relative percentage distribution of burst durations for two age groups with the 65th percentile threshold at representative channel CP3 (see Section 2.3.5.). Statistics (Wilcoxon rank sum test) showed that compared to the young group, elderly subjects showed a tendency for bursts with longer duration windows (0.2–0.5 s). The percentage of shorter beta bursts (0.1–0.2 s) was higher in young compared to elderly subjects ($^*p$ = 0.0122, after FDR). In contrast, across the nine burst duration windows, the percentage of relatively longer bursts in a given interval (0.2–03 s, 0.3–0.4 s, 0.4–0.5 s) was higher in the elderly group ($^*p$ = 0.0132, $^*p$ = 0.0132, $^*p$ = 0.0184, respectively, FDR corrected) compared to the young group. However, for the longer bursts lasting more than 0.5 s we did not observe any difference between the groups. Moreover, the relative number of the bursts in intervals (> 0.5 s) was much smaller compared to bursts lasting less than 0.5 s. These results showed that in the resting state EEG of the aged brain, beta rhythm commonly appears with a duration of around 2–6 cycles, with a few portions of bursts lasting ~10 cycles and rarely with a longer duration time (> 10 cycles). In order to investigate a spatial pattern of this effect, we categorized the windows into two categories, namely short windows (0.1–0.2 s) and long windows (0.2–0.5 s). Next, we compared the percentages of bursts with long windows

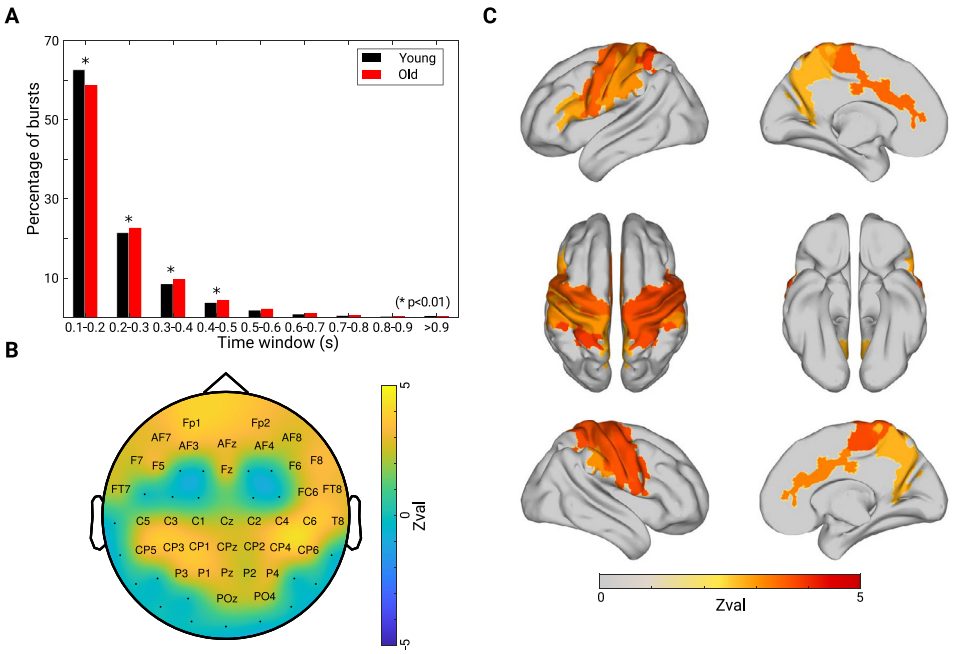

Fig. 5. Changes in burst duration distribution. A. The relative number of bursts in each bin is given as a percentage of the total number of bursts. The bar graph shows the mean of each age group across burst events with different bin duration at representative electrode CP3. For both groups, with increasing burst duration the percentage of bursts decreases. Elderly subjects had a lower percentage of short bursts (burst window: 0.1–0.2 s) (*p = 0.0122, after FDR) and larger percentage of long bursts (burst window: 0.2–0.3, 0.3–0.4,0.4–0.5 s) (*p = 0.0132, 0.0132, 0.0184, respectively, after FDR) compared to young subjects. B. Scalp topography of differences (old vs. young) in percentages of long burst (0.2–0.5 s). Labeled electrodes are those showing significantly higher percentage of long bursts in elderly than in young subjects after FDR correction ($p < 0.05$). C. Spatial difference pattern in the percentage of long bursts (old vs. young) in source level. Positive values indicate larger values in the group with elderly subjects.

between the two groups for all channels. In Fig. 5B, we plotted the topographical pattern of the difference in relative number of beta bursts with long duration between two age groups. The cortical areas demonstrating strongest age-related beta burst differences are clustered over bilateral frontal and centro-parietal sites. Additionally, the analysis in source space further located the spatial difference pattern mostly in the bilateral sensorimotor cortices (Fig. 5C). To demonstrate how overall differences in burst duration and amplitude between two groups converge across various threshold percentiles for definition of beta burst event, we analyzed these two key parameters across a family of nine thresholds from the 50th to 90th percentiles (see supplemental analysis 3 and Figure S5). The analysis showed that generally the elderly subjects have longer beta burst events together with higher amplitude, regardless of the threshold definition. Additionally, we obtained similar results for this part of analysis with a different threshold for burst definition, i.e., 70th percentile (see Figure S8 in supplemental material).

3.2.2. Incidence rate of bursts with long duration is increased in elderly subjects

In addition, we investigated how often beta bursts occur with a given duration window. Burst incidence rate was calculated as the number of beta bursts per second. We compared the burst incidence rate for all windows across all channels. We found that there is no difference in incidence rate for shorter windows (0.1–0.2 s) between two groups, whereas for the longer windows (0.2–0.3 s, 0.3–0.4 s, 0.4–0.5 s) the incidence rates showed an increase in a region specific pattern in the elderly compared to the young group. The result for each window is shown in Fig. 6A. Specifically, for bursts with a duration 0.2–0.3 s, the frequency of bursts increased with most prominent changes occurring in frontocentral regions. The regions showing significant differences were more focally clustered for longer bursts (> 0.3 s). For the relatively longer 0.4–0.5 s window, the prominent difference was present in a small cluster of regions over centro-parietal sites. Furthermore, Fig. 6B shows a spatial difference pattern in source space. Burst incidence rate was averaged over all the bursts with long duration windows (0.2–0.5 s) and compared across all brain areas between the two groups (old vs. young). The pattern showed significant differences after FDR correction. With this analysis we further confirmed that the elderly subjects, compared to young subjects, were indeed characterized by more frequent long beta burst events, which occurred in multiple cortical regions but most prominently in bilaterally pre- and post-central gyri. To show the distribution of the incidence of bursts for all channels and subjects in different groups regardless of window duration, we additionally obtained the mean burst incidence for each channel by averaging the burst incidence rate across the three above-mentioned windows, and then plotted a corresponding normalized histogram (see Fig. 6C). A trend was observed for the higher incidence rate in the elderly group in comparison to the young subjects.

3.3. Relationship between PAC and beta burst dynamics

Finally, to investigate whether PAC and bursts characteristics relate to the same neuro-physiological mechanism, we investigated a correlation between them topographically within each age group (PAC versus percentage of beta bursts with specific intervals showing the largest differences between the groups (short window of 0.1–0.2 s and mean of long windows of 0.2–0.5 s)), results are shown in Fig. 7. Spearman's correlations were performed for all channels and across all the subjects for young and old group, respectively. For the young group, there was no significant relationship between PAC and percentage of short bursts or long bursts. As shown in Fig. 7, the percentage of bursts with short (0.1–0.2 s, Fig. 7A) and long durations (0.2–0.5 s, Fig. 7B), were significantly related to PAC values only in a small cluster of electrodes primarily located in right frontal area in the elderly group. Specifically, PAC was positively correlated with the percentage of short bursts (Fig. 7A), and the opposite was observed for long bursts (Fig. 7B). Spatial correlation maps were distinct from those corresponding to PAC differences (Fig. 3) and beta burst differences (Fig. 5), thus suggesting that the PAC and beta bursts are likely to reflect distinct processes in healthy aging. In order to further localize the source of correlation map that we observed in sensor space, we performed correlation analysis similarly on metrics estimated from the signal reconstructed in the source space. Specifically, for each ROI, PAC and burst percentage (short and longer bursts) was estimated and then correlation analysis was performed across the subjects within the elderly group for all the ROIs. Before applying FDR correction, for the short bursts (0.1–0.2 s), strongest positive relations were observed in bilateral cingulate gyri, and left occipital pole. And analogously the strongest negative correlations were present in the bilateral cingulate gyri, left superior frontal gyrus and right insula cortex between longer burst (0.2–0.5 s) and PAC. After applying correction for multiple com-

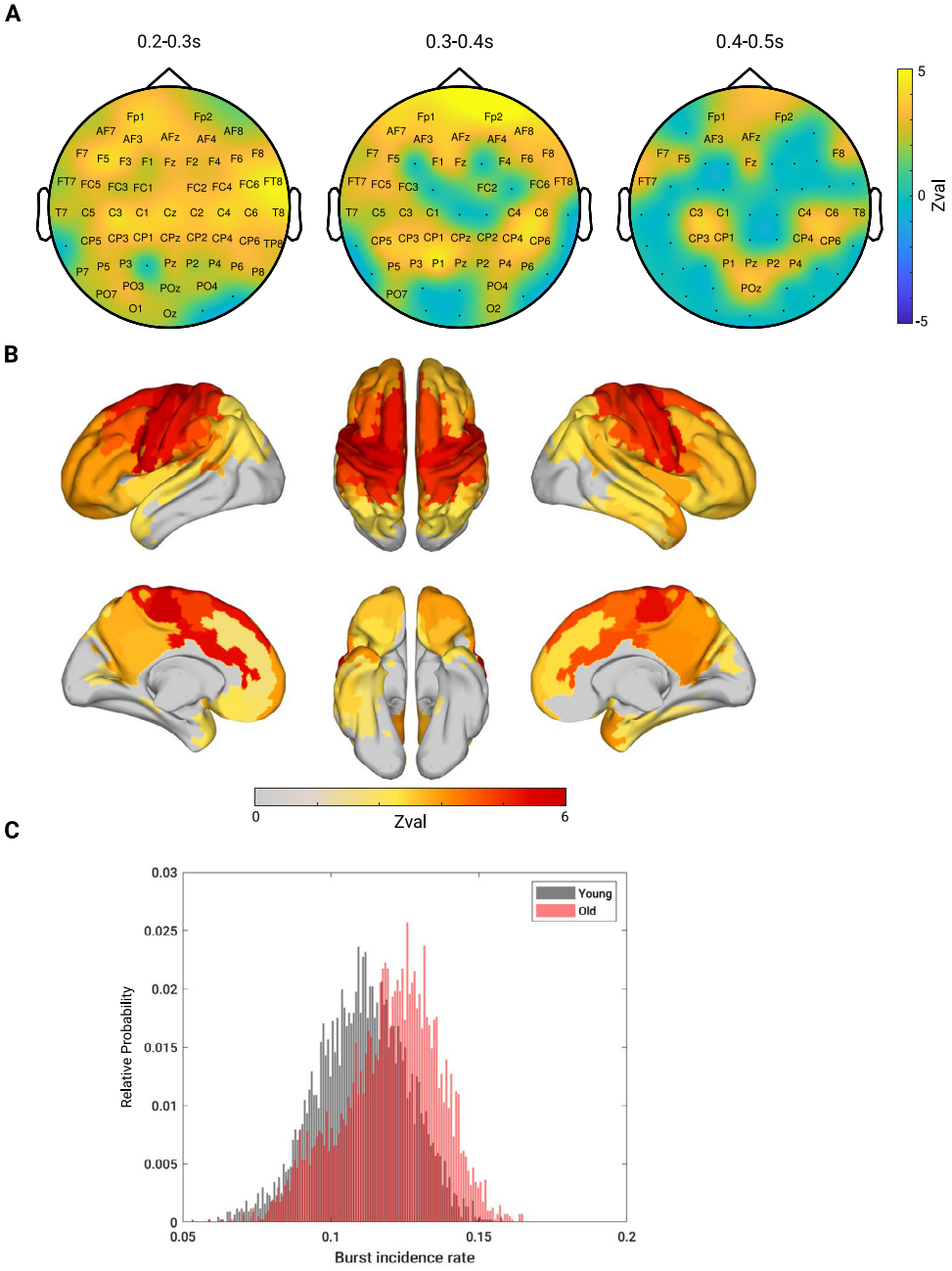

Fig. 6. Changes in incidence rate of longer duration windows (0.2–0.5 s) (old vs. young). A. Spatial topography of the difference in incidence rates of bursts with different durations. Electrodes with labels showed significant difference between the two groups (old vs. young) after FDR correction ($p < 0.05$). For bursts with a duration of 0.2–0.3 s, a significant increase was observed in many scalp sites but most prominently in fronto-central regions. For bursts with a duration between 0.4 and 0.5 s, the most prominent differences were found in centro-parietal areas. B. Spatial difference pattern (old vs. young) in burst incidence rate of long beta bursts (0.2–0.5 s) in source level. C. Normalized histogram of mean incidence rates of longer bursts (0.2–0.5 s) across all channels and subjects for the old (in red) and young (in black) group. Each count represents one channel from one subject. Color bar indicates the test statistic. Positive values indicate stronger bursting incidence in the elderly subjects.

parisons, none of the significance remained. The lack of significant relations between these two measures estimated in the source space may further support the idea that these two parameters might reflect different aspects of healthy aging.

4. Discussion

Despite previous clinical evidence in support of a close association between aging and PD, electrophysiological neuronal correlates of such an association have been rather elusive. Here, we showed that the electrophysiological biomarkers recently discovered for PD, are also present in apparently healthy elderly subjects. Specifically, we found the elevated PAC and more frequent beta bursts with longer duration being pronounced in the elderly group compared to the young one. Importantly, such differences were particularly manifested in sensorimotor areas. Furthermore, we found only a weak correlation between PAC and beta bursts metrics, suggesting that these phenomena may reflect different aspects of healthy aging. Overall, our findings indicate that electrophysiological alterations detected in PD already exist in the apparently healthy aging brain and their further amplification may eventually manifest in clinical symptoms typically found in fully developed PD.

4.1. Topography of PAC changes in the healthy aging brain

PAC has been increasingly suggested to be a biomarker for pathology in PD, being a proxy for the locking of local spiking activity to beta oscillation within and across the basal ganglia-cortical network (De Hemptinne et al., 2015; Malekmohammadi et al., 2018; Swann et al., 2015; Weinberger et al., 2006). Although we were initially interested in testing the assumption that during apparently healthy aging an increase in PAC between beta band (13–30 Hz) and broadband gamma activity

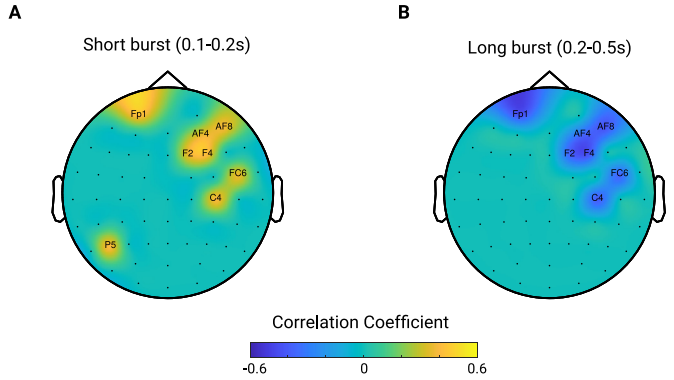

Fig. 7. Correlation maps between PAC values and percentage of burst with short and long durations. A. Correlation map between PAC and percentage of short bursts (0.1–0.2 s) within elderly group. B. Correlation between PAC values and long bursts (0.2–0.5 s) across all subjects within elderly group. The significance is indicated after applying FDR-correction across multiple comparisons for all the channels.

(50–150 Hz) could be observed over the sensorimotor cortex, as it has been repeatedly indicated in previous PD studies using ECoG or EEG (A. M. Miller et al., 2019; De Hemptinne et al., 2013; Jackson et al., 2019; Swann et al., 2015), we nonetheless investigated changes in PAC over the whole cortex. Given a premise that PAC in elderly subjects can resemble behavior of PAC in patients with PD, our results confirmed previous findings showing that PAC is primarily increased over the sensorimotor areas. This is in agreement with previous studies showing age-related alterations in cortical motor areas (Haug and Eggers, 1991; Ward and Frackowiak, 2003), as well as changes in the functioning of these areas (C. Clark and L. Taylor, 2012; Fathi et al., 2010; Heuninckx et al., 2005; Michely et al., 2018; Rowe et al., 2006). In addition, we also observed stronger differences over the left hemisphere. Such hemispheric asymmetry in PAC might relate to the stronger dopaminergic defect in the dominant compared to the non-dominant hemispheres defined by a subject's dominant hand, one of the major factors causing PD symptoms to emerge more often on the dominant hand-side (Shi et al., 2014). In our dataset, the majority of subjects are right-handed (129 out of 137).

Cortical broadband gamma is thought to reflect asynchronous spiking activity (K. J. Miller et al., 2009; Manning et al., 2009). Therefore, elevated coupling of beta and broadband gamma activity can represent a higher synchronization of local spiking activity to the phase of beta oscillation. Excessive PAC in the aging brain may reflect a physiological state in which the cortex is restricted to more rigid activity patterns, rendering it less able to respond dynamically to signals from higher order cortical regions. Such dynamic inflexibility is in line with previous studies, showing that aging is accompanied by decreased neuronal complexity estimated with fractal dimension using resting state measures of neuronal activity (Zappasodi et al., 2015). In addition, fMRI studies have also shown a lower level of spontaneous BOLD signal variability (another frequently used measure of neuronal complexity) in older subjects (Grady and Garrett, 2014; Kumral et al., 2020; Nomi et al., 2017).

4.2. Cortical beta bursts in the healthy aging brain

Beta oscillations are associated with prefrontal working memory (Lundqvist et al., 2011, 2018), stopping action and thought (Michelmann et al., 2016; Wessel and Aron, 2017), and most widely – to sensorimotor function (Baker, 2007; Espenhahn et al., 2019; Feingold et al., 2015; Gehringer et al., 2018; Pfurtscheller et al., 1996; Pollok et al., 2014). Age-related increase in beta band power over the bilateral sensorimotor cortices has been reported in previous studies (Heinrichs-Graham and Wilson, 2016), consistent with that which we observed in our study (see supplemental analysis 1.2 and Figure S2). As beta power has been linked to the level of inhibitory GABAergic neural transmission, age related increase of beta power at baseline may suggest increased intracortical GABAergic inhibition (Rossiter et al., 2014).

Beta activity is characterized by short-lived burst events (Feingold et al., 2015; Murthy and Fetz, 1992; Sherman et al., 2016), instead of a continuous oscillatory pattern. Importantly, beta bursts have been investigated in the STN in PD studies which showed longer burst duration and increase of incidence rate in OFF compared to ON levodopa state (Tinkhauser et al., 2017b). Moreover, movement-associated reduced incidence rate and amplitude of bursts contributed to the pathological decrease of movement velocity (Lofredi et al., 2019) in PD patients. These distinct functional roles of transient beta events indicate the importance of episodic nature of beta bursts in flexible coordination of responses in tasks. In our study we extended previous findings to spontaneous resting state brain activity measured from scalp EEG, confirming the transient nature of cortical beta events. Furthermore, we demonstrated an age-related increase in the duration and occurrence of beta bursts in a region-specific pattern. Such re-distribution of burst duration to longer windows together with an increased occurrence of longer bursts may compromise the flexible coordination of brain dynamics, especially in motor processing, reflected in a central motor clustered spatial pattern.

The mechanistic origin of neocortical beta burst events was investigated in detail in the work of (Sherman et al., 2016). Their simulation results have shown that beta events could emerge from nearly synchronous bursts of excitatory synaptic drive targeting proximal and distal dendrites of pyramidal neurons in the cortex. Additionally, they suggested that the ventral medial/pallidal thalamus was particularly well suited for this distal drive. Importantly, the ventromedial (VM)/pallidal thalamus project dominantly and diffusely to the supragranular layers in the sensory and motor cortex as well as the prefrontal cortex, which is quite consistent with the spatial distribution in beta burst duration changes observed in our study (see Fig. 5B). This might lead to the assumption that thalamo-cortical loops of motor related pathway are a fundamental component in generation and age-related alteration in cortical beta burst dynamics. More frequent and longer beta bursts are probably due to the increased drive from the thalamus, which has been shown to be affected by age through complex changes in macrostructure, microstructure and neural connectivity (Fama and Sullivan, 2015). Meanwhile, cortical beta bursts could also be generated independently in the STN-Gpe (external globus pallidus) network within the basal ganglia (Kumar et al., 2011) and propagate via thalamo-cortical loops to the cortex (McFarland and Haber, 2002).

In fact, a very recent study revealed a possible mechanism of propagation of beta bursts within the cortical-basal ganglia circuit in PD (Cagnan et al., 2019). The authors showed an association between cortical and basal ganglia beta bursts, when especially longer cortical beta bursts were associated with longer periods of increased beta amplitude in GPe following the burst onset. This is in line with a previous study showing that cortical beta changes preceded changes in sub-cortical regions, suggesting an important role for cortical feedback in maintaining pathological basal ganglia oscillations (De Hemptinne et al., 2013). Additionally, it has also been reported that the effective STN-DBS treatment not only modulates the local STN beta oscillations, but also attenuates the coherence between motor cortices and the STN (Oswal et al., 2016). These findings suggest that pathological coupling across nodes (cortical and sub-cortical) in the basal ganglia-thalamo-cortical (BGTC) network might play an important role in motor function impairment. Moreover, in the present study, we showed that cortical sensorimotor beta dynamics were also modulated due to physiological aging. This in turn indicates that cortical beta dynamics might serve as a proxy for the coordination of structures within the motor related network and underlie physiological and pathological changes.

4.3. Relationship between different measures of PAC and beta burst in healthy aging

Both PAC and beta bursts in the STN have previously been linked to symptom severity in PD. Dopamine replacement in PD patients suppresses both burst length (Cagnan et al., 2015; Tinkhauser et al., 2017b) and PAC (López-Azcárate et al., 2010; van Wijk et al., 2016). However, how these two different phenomena relate to each other remains rather elusive. To our best knowledge, one recent paper studied PAC during periods of beta bursting using macro and micro electrode recordings in the STN in PD patients (Meidahl et al., 2019). The authors provide converging evidence demonstrating that the coupling of spiking to the network beta oscillations is significantly higher during beta bursts and increases progressively with beta burst duration. Therefore, the authors suggested that PAC and beta bursts might reflect similar neurophysiology due to excessive synchronization. More recently, one study using ECOG at M1 demonstrated PAC was more pronounced during periods of beta burst than non-bursts in PD, but without showing significant difference between PD and non-PD groups during bursts (O'Keeffe et al., 2020). In our resting EEG study, we also showed significantly elevated PAC and prolonged beta bursts with more frequent occurrence in healthy elderly compared to young subjects. We acknowledge that higher PAC is very likely to occur during episodes of beta bursts since a higher signal-to-noise ratio may play a critical role, which is, nevertheless, challenging to disentangle. However, by investigating an association between PAC and beta bursts features within each age group in a topographical manner with multichannel EEG, we found no spatial overlap between them, except for the focally distributing right frontal region (AF4, AF8, F2, F4) and several other isolated channels in the elderly group. In addition, by localizing the signal in the source space none of the cortical regions showed a significant correlation. We therefore suggest that in healthy aging, at the level of cortex PAC and beta burst dynamics may reflect rather different neurophysiological processes.

4.4. PD: accelerated aging phenomenon?

Aging and PD related brain alterations share similarities (G. Levy, 2007; Pang et al., 2019; Reeve et al., 2014). They can be manifested at the level of cellular mechanisms where dopamine cellular risk factors accumulate with age in a pattern which mimics the pattern of dopamine degeneration in PD based on the evidence from studies of non-human primates (Collier et al., 2011). Moreover, the evidence from midbrain dopamine neurons of aging non-human primates further supported that the view that age-related changes in the dopamine system approach the biological threshold for parkinsonism (Collier et al., 2017).

Zeighami et al. (2019) used a data driven approach to investigate anatomical brain signatures of PD. In their first identified latent variable, age was the strongest contributor to brain atrophy. Further, in a longitudinal study, they showed that both healthy aging and PD were associated with cortical thinning over a one-year period, but with a more prominent alteration in PD patients than in healthy controls (Yau et al., 2018). This again demonstrates a similar directionality of alteration in aging and PD in terms of cortical anatomy. Age remains the largest risk factor for many diseases and in our study we showed that it can also be associated with electrophysiological biomarkers of PD. Importantly, our results demonstrated that not in all elderly subjects we observed increased PAC and longer beta bursts, which in turn indicates that other factors such as genes, life style, environment and other factors shape the corresponding neuronal processes and account for the individual variations.

Further, to address to what degree our estimated effects in healthy aging relate to the previously reported PD biomarkers, we compared them in rather a qualitative manner since factors such as the recording setup, data length and signal-processing steps could result in a different scale of the estimated metrics. With respect to the spectral and spatial overlap of PAC in healthy aging and PD, we refer here to three previous studies in PD in which spatial distributions were provided offering a chance to have a general comparison. In the studies by Swann et al. (2015) and A. M. Miller et al. (2019), one could see a prominent PAC region over beta and further lower gamma phase frequency ranges (their Fig. 2A) and a slightly prominent cluster region over beta phase frequency (their Fig. 2A) in the PD Off-medication group, respectively. In a very recent paper, the authors also showed a pronounced PAC pattern over beta phase frequency in patients with PD compared to healthy controls (see their Fig. 2B) (Gong et al., 2021). However, since in all these studies there was no cluster-based permutation test or demonstration to which phase frequency the amplitude from broadband gamma was phase locked to, we may only draw the conclusion that the beta band phase modulating PAC in the current study, to a large extent, overlaps with the frequency range presented in previous studies. Regarding the spatial distribution, from the Fig. 5B from the first study (Swann et al., 2015) and Fig. 3B from the second one (A. M. Miller et al., 2019), together with what has been observed in the current study (Fig. 3A), one can see that the left central regions are consistently found in all three studies. In addition, in the study Gong et al. (2021) the authors averaged the data from the two hemispheres and the area with the largest differences was localized mainly in the sensorimotor region (premotor cortex (PMC) and primary motor cortex (M1)). Comparing the beta burst properties to that in the study by Tinkhauser et al. (2017b), we found that although in healthy aging a relatively larger percentage of longer bursts was observed, there was no difference in terms of the very long bursts, for instance bursts longer than 0.5 s. The other difference is that in the LFP of STN in PD during off medication, the percentage of bursts longer than 900 ms is abnormally high. The mean of the burst duration in PD off medication is thus higher than what we observed in healthy aging subjects and after the medication the mean duration dropped to less than 0.3 s which is comparable to the results from the healthy elderly participants in our study. In a recently published study using ECoG over motor cortices, the authors showed that in the motor cortex of patients with PD, a relative increase of beta burst duration was demonstrated in comparison to the patients with essential tremor (O'Keeffe et al., 2020). Comparing our results to their Fig. 2B, we note that the mean duration of beta bursts in PD (around 0.2 s) is indeed more comparable to that from healthy elderly in the current study. Importantly, our findings regarding the burst features were well localized in the bilateral motor cortices (pre- and post- central gyri, see Fig. 5C and Fig. 6B). In conclusion, PAC features obtained in the present study largely overlap in frequency and spatial content in both aging and PD processes. Moreover, the effect of beta burst dynamics in healthy aging shows the same direction with that of PD during off state compared to the state after effective therapy (DBS or medication) or to the patients with essential tremor (instead of comparing to healthy controls), and it is commonly reported in the cortical motor region.

4.5. Potential non-invasive electrophysiological biomarker for detection of parkinsonian state

Early diagnosis of potential PD development is crucial for effective clinical intervention. Here, we provide evidence that the altered PAC and beta bursts are associated with aging in a manner similar to PD. Moreover, we conducted a correlation analysis between PAC and beta bursts across the whole scalp and cortical areas, and did not find a strong relationship between them. Therefore, we suggest that a combination of these two different metrics may lead to a more comprehensive estimation of age-related changes in the brain potentially culminating in the development of clinical symptoms typical for PD.

We have linked apparently healthy aging and PD by investigating electrophysiological signatures in a cross-sectional way. These non-invasive metrics might be helpful in estimating a proximity of neuronal dynamics relating to parkinsonian state. A recent study examined changes in cortical PAC in a progressive model of parkinsonism (Devergnas et al., 2019). Although the authors reported that cortical

PAC only reached significance when the animals became fully parkinsonian, their results showed a trend towards increased PAC in parallel with the development of parkinsonism. In the present study, although we did not find differences in TAP reaction times in elderly participants with high and low PAC values, a future prospective study may identify that participants with particularly strong PAC are more likely to develop parkinsonian symptoms. In this study, we observed in the elderly group, that there was a trend of increasing correspondence between PAC and age-related behavioral reaction times. Importantly, this relationship was not present in the young group. This may provide a hint regarding the functional relevance of the PAC increase in healthy aging, which might be related to a reduced readiness of the motor system to be engaged in the production of movements. Although we regard this as an interesting finding, we refrain from drawing a strong conclusion from it since these behavioral data are not a straightforward measure of movement performance.

Clearly, an objective set of criteria is needed to define a threshold for normal or abnormal brain aging. For this purpose, we suggest that longitudinal studies in which motor performance is specifically measured to be an indicative of potential parkinsonian state, measuring EEG over a long period, for instance 5–20 years, starting already in the middle age could provide additional information on the progression of PAC and beta burst dynamics in relation to possible development of parkinsonian symptoms. By combining both approaches, we may better identify a turning-point indicating a disruption of apparently healthy aging course, potentially relating to pathological aging process. Finally, applying interventions, such as medication or early non-invasive brain stimulation during sleep (Romanella et al., 2020), before healthy aging switches to a pathological trajectory might slow down or even restore pathological neural alterations relating to the development of PD.

5. Limitations

The first limitation of the study is that it was not based on the direct comparison of the EEG parameters obtained in cohorts of patients with PD and healthy subjects with aging. Besides, a comparison to the previous literature quantitatively is difficult since those studies have different settings such as cap electrodes density, postural condition, recording time length etc. Yet our main idea related to the effect of aging on EEG characteristics typically associated with PD. Certainly for further applicability of our findings to PD, patients should be recruited.

Furthermore, although we have performed a careful cleaning of the data based on ICA and removal of noisy segment via visual inspection, some residual artifacts might still be present. This is especially relevant for high gamma activity which lies in the frequency range of artifactual muscle activity. However, our source analysis has shown that the main differences in PAC between two groups of participants were over sensorimotor areas rather than over the temporal areas where one would expect the largest contribution from scalp muscles. Additionally, we provide further extensive discussion on the relevance of muscle activity for PAC effect (see supplemental discussion 2.). We would also like to note that due to the limitations of non-invasive recordings, we can't rule out completely the effect of residual muscle activity on the generation of PAC. Future studies, utilizing direct invasive measurement of cortical activity, should be more informative about such influence.

In our study, we applied standard head modeling and ROIs based analysis in the source space. More precise estimates could be obtained if the analysis is performed with individual head models. Yet, in our study we used a relatively large number of ROIs which at least partially negates a lack of spatial accuracy.

Conclusion

In this study, using resting state EEG, we found that apparently healthy aging is associated with the cortical neuronal signatures resembling those typically found in patients with PD. The differences in PAC and in the burst characteristics of beta oscillations between elderly and young subjects exhibited distinct spatial patterns with a considerable presence over sensorimotor areas of the cortex. Aging related changes in PAC and beta burst dynamics share the directionality with that characterizing PD. Such a similarity may suggest that the electrophysiological signatures typically found in PD might already be detectable in the apparently healthy aging brain. Consequently we assume that further exaggeration of such neuronal changes may eventually result in the development of motor abnormalities typical for PD. Furthermore, once established and validated in other studies, the investigated metrics may have potential to serve as the biomarkers for the early detection of the gradually developing neuronal changes characterizing pre-parkinsonian state. Finally, our findings highlight the importance of adequate control for aging effects in PD studies via the inclusion of both patients and healthy controls.

Acknowledgments

We are grateful to Ruxue Gong for discussions on the data analysis. This work was supported in part by Deutsche Forschungsgemeinschaft (German Research Foundation) (Project ID: 424778381 TRR 295). JZ was supported by China Scholarship Council (CSC). VVN was supported in part by the Basic Research Program at the National Research University Higher School of Economics.

Data and code availability statement

EEG data are from a public dataset which was acquired by Babayan et al. (2019). The codes used for some key data analyses are publicly available via GitHub: https://github.com/JuanliZhang/PAC.

Supplementary materials

Supplementary material associated with this article can be found, in the online version, at doi:10.1016/j.neuroimage.2021.118512.

References

Babayan, A., Erbey, M., Kumral, D., Reinelt, J.D., Reiter, A.M.F., Röbbig, J., Lina Schaare, H., Uhlig, M., Anwander, A., Bazin, P.L., Horstmann, A., Lampe, L., Nikulin, V.V., Okon-Singer, H., Preusser, S., Pampel, A., Rohr, C.S., Sacher, J., Thöne-Otto, A., …, Villringer, A., 2019. Data descriptor: a mind-brain-body dataset of MRI, EEG, cognition, emotion, and peripheral physiology in young and old adults. Sci. Data 6, 1–21. doi:10.1038/sdata.2018.308.

Baker, S.N., 2007. Oscillatory interactions between sensorimotor cortex and the periphery. Curr. Opin. Neurobiol. 17 (6), 649–655. doi:10.1016/j.conb.2008.01.007.

Brittain, J.S., Sharott, A., Brown, P., 2014. The highs and lows of beta activity in cortico-basal ganglia loops. Eur. J. Neurosci. 39 (11), 1951–1959. doi:10.1111/ejn.12574.

Brown, P., 2003. Oscillatory nature of human basal ganglia activity: relationship to the pathophysiology of parkinson's disease. Mov. Disord. 18 (4), 357–363. doi:10.1002/mds.10358.

Clark, C., B., Taylor, L., J., 2012. Age-related changes in motor cortical properties and voluntary activation of skeletal muscle. Curr. Aging Sci. 4 (3), 192–199. doi:10.2174/1874609811104030192.

Cagnan, H., Duff, E.P., Brown, P., 2015. The relative phases of basal ganglia activities dynamically shape effective connectivity in Parkinson's disease. Brain 138 (6), 1667–1678. doi:10.1093/brain/awv093.

Cagnan, H., Mallet, N., Moll, C.K.E., Gulberti, A., Holt, A.B., Westphal, M., Gerloff, C., Engel, A.K., Hamel, W., Magill, P.J., Brown, P., Sharott, A., 2019. Temporal evolution of beta bursts in the parkinsonian cortical and basal ganglia network. PNAS 116 (32), 16095–16104. doi:10.1073/pnas.1819975116.

Chen, C.C., Hsu, Y.T., Chan, H.L., Chiou, S.M., Tu, P.H., Lee, S.T., Tsai, C.H., Lu, C.S., Brown, P., 2010. Complexity of subthalamic 13-35Hz oscillatory activity directly correlates with clinical impairment in patients with Parkinson's disease. Exp. Neurol. 224 (1), 234–240. doi:10.1016/j.expneurol.2010.03.015.

Cheng, H.C., Ulane, C.M., Burke, R.E., 2010. Clinical progression in Parkinson disease and the neurobiology of axons. Ann. Neurol. 67 (6), 715–725. doi:10.1002/ana.21995.

Cole, S.R., van der Meij, R., Peterson, E.J., de Hemptinne, C., Starr, P.A., Voytek, B., 2017. Nonsinusoidal beta oscillations reflect cortical pathophysiology in parkinson's disease. J. Neurosci. 37 (18), 4830–4840. doi:10.1523/JNEUROSCI.2208-16.2017.

Collier, T.J., Kanaan, N.M., Kordower, J.H., 2011. Ageing as a primary risk factor for Parkinson's disease: evidence from studies of non-human primates. Nat. Rev. Neurosci. 12 (6), 359–366. doi:10.1038/nrn3039.

Collier, T.J., Kanaan, N.M., Kordower, J.H., 2017. Aging and Parkinson's disease: different sides of the same coin? Mov. Disord. 32 (7), 983–990. doi:10.1002/mds.27037.

Crowell, A.L., Ryapolova-Webb, E.S., Ostrem, J.L., Galifianakis, N.B., Shimamoto, S., Lim, D.A., Starr, P.A., 2012. Oscillations in sensorimotor cortex in movement disorders: an electrocorticography study. Brain 135 (2), 615–630. doi:10.1093/brain/awr332.

Darden, L., 2007. Mechanisms and models. Cambridge Companion Philos. Biol. 39, 139–159. doi:10.1017/CCOL9780521851282.008.

De Hemptinne, C., Ryapolova-Webb, E.S., Air, E.L., Garcia, P.A., Miller, K.J., Ojemann, J.G., Ostrem, J.L., Galifianakis, N.B., Starr, P.A., 2013. Exaggerated phase-amplitude coupling in the primary motor cortex in Parkinson disease. PNAS 110 (12), 4780–4785. doi:10.1073/pnas.1214546110.

De Hemptinne, C., Swann, N.C., Ostrem, J.L., Ryapolova-Webb, E.S., Luciano, San, M., Galifianakis, N., B., Starr, P.A, 2015. Therapeutic deep brain stimulation reduces cortical phase-amplitude coupling in Parkinson's disease. Nat. Neurosci. 18 (5), 779–786. doi:10.1038/nn.3997.

Delorme, A., Makeig, S., 2004. EEGLAB: an open source toolbox for analysis of single-trial EEG dynamics including independent component analysis. J. Neurosci. Methods 134 (1), 9–21. doi:10.1016/j.jneumeth.2003.10.009.

Desikan, R.S., Ségonne, F., Fischl, B., Quinn, B.T., Dickerson, B.C., Blacker, D., Buckner, R.L., Dale, A.M., Maguire, R.P., Hyman, B.T., Albert, M.S., Killiany, R.J., 2006. An automated labeling system for subdividing the human cerebral cortex on MRI scans into gyral based regions of interest. Neuroimage 31 (3), 968–980. doi:10.1016/j.neuroimage.2006.01.021.

Devergnas, A., Caiola, M., Pittard, D., Wichmann, T., 2019. Cortical phase-amplitude coupling in a progressive model of Parkinsonism in nonhuman primates. Cereb. Cortex 29 (1), 167–177. doi:10.1093/cercor/bhx314.

Espenhahn, S., van Wijk, B.C.M., Rossiter, H.E., de Berker, A.O., Redman, N.D., Rondina, J., Diedrichsen, J., Ward, N.S., 2019. Cortical beta oscillations are associated with motor performance following visuomotor learning. Neuroimage 195 (February), 340–353. doi:10.1016/j.neuroimage.2019.03.079.

Eusebio, A., Thevathasan, W., Doyle Gaynor, L., Pogosyan, A., Bye, E., Foltynie, T., Zrinzo, L., Ashkan, K., Aziz, T., Brown, P., 2011. Deep brain stimulation can suppress pathological synchronisation in parkinsonian patients. J. Neurol., Neurosurg. Psychiatry 82 (5), 569–573. doi:10.1136/jnnp.2010.217489.

Eusebio, Alexandre, Brown, P., 2009. Synchronisation in the beta frequency-band - the bad boy of Parkinsonism or an innocent bystander? Exp. Neurol. 217 (1), 1–3. doi:10.1016/j.expneurol.2009.02.003.

Fama, R., Sullivan, E.V., 2015. Thalamic structures and associated cognitive functions: relations with age and aging. Neurosci. Biobehav. Rev. 54, 29–37. doi:10.1016/j.neubiorev.2015.03.008.

Fathi, D., Ueki, Y., Mima, T., Koganemaru, S., Nagamine, T., Tawfik, A., Fukuyama, H., 2010. Effects of aging on the human motor cortical plasticity studied by paired associative stimulation. Clin. Neurophysiol. 121 (1), 90–93. doi:10.1016/j.clinph.2009.07.048.

Feingold, J., Gibson, D.J., Depasquale, B., Graybiel, A.M., 2015. Bursts of beta oscillation differentiate post performance activity in the striatum and motor cortex of monkeys performing movement tasks. PNAS 112 (44), 13687–13692. doi:10.1073/pnas.1517629112.

Gehringer, J.E., Arpin, D.J., Heinrichs-Graham, E., Wilson, T.W., Kurz, M.J., 2018. Neurophysiological changes in the visuomotor network after practicing a motor task. J. Neurophysiol. 120 (1), 239–249. doi:10.1152/jn.00020.2018.

Gong, R., Wegscheider, M., Mühlberg, C., Gast, R., Fricke, C., Rumpf, J.J., Nikulin, V.V., Knösche, T.R., Classen, J., 2021. Spatiotemporal features of β-γ phase-amplitude coupling in Parkinson's disease derived from scalp EEG. Brain : J. Neurol. 144 (2), 487–503. doi:10.1093/brain/awaa400.

Grady, C.L., Garrett, D.D., 2014. Understanding variability in the BOLD signal and why it matters for aging. Brain Imaging Behav. 8 (2), 274–283. doi:10.1007/s11682-013-9253-0.

Hammond, C., Bergman, H., Brown, P., 2007. Pathological synchronization in Parkinson's disease: networks, models and treatments. Trends Neurosci. 30 (7), 357–364. doi:10.1016/j.tins.2007.05.004.

Haufe, S., Ewald, A., 2016. A Simulation Framework for Benchmarking EEG-Based Brain Connectivity Estimation Methodologies. Brain Topography.

Haug, H., Eggers, R., 1991. Morphometry of the human cortex cerebri and corpus striatum during aging. Neurobiol. Aging 12 (4), 336–338. doi:10.1016/0197-4580(91)90013-A.

Heinrichs-Graham, E., Wilson, T.W., 2016. Is an absolute level of cortical beta suppression required for proper movement? Magnetoencephalographic evidence from healthy aging. Neuroimage 134, 514–521. doi:10.1016/j.neuroimage.2016.04.032.

Heuninckx, S., Wenderoth, N., Debaere, F., Peeters, R., Swinnen, S.P., 2005. Neural basis of aging: the penetration of cognition into action control. J. Neurosci. 25 (29), 6787–6796. doi:10.1523/JNEUROSCI.1263-05.2005.

Hindle, J.V., 2010. Ageing, neurodegeneration and Parkinson's disease. Age Ageing 39 (2), 156–161. doi:10.1093/ageing/afp223.

Huang, Y., Parra, L.C., Haufe, S., 2016. The New York Head—a precise standardized volume conductor model for EEG source localization and tES targeting. Neuroimage 140, 150–162. doi:10.1016/j.neuroimage.2015.12.019.

Jackson, N., Cole, S.R., Voytek, B., Swann, N.C., 2019. Characteristics of waveform shape in Parkinson's disease detected with scalp electroencephalography. ENeuro 6 (3), 1–11. doi:10.1523/ENEURO.0151-19.2019.

Kim, S., Myers, L., Wyckoff, J., Cherry, K.E., Jazwinski, S.M., 2017. The frailty index outperforms DNA methylation age and its derivatives as an indicator of biological age. GeroScience 39 (1), 83–92. doi:10.1007/s11357-017-9960-3.

Kramer, M.A., Tort, A.B.L., Kopell, N.J., 2008. Sharp edge artifacts and spurious coupling in EEG frequency comodulation measures. J. Neurosci. Methods 170 (2), 352–357. doi:10.1016/j.jneumeth.2008.01.020.

Kühn, A.A., Tsui, A., Aziz, T., Ray, N., Brücke, C., Kupsch, A., Schneider, G.H., Brown, P., 2009. Pathological synchronisation in the subthalamic nucleus of patients with Parkinson's disease relates to both bradykinesia and rigidity. Exp. Neurol. 215 (2), 380–387. doi:10.1016/j.expneurol.2008.11.008.

Kumar, A., Cardanobile, S., Rotter, S., Aertsen, A., 2011. The role of inhibition in generating and controlling Parkinson's disease oscillations in the basal ganglia.. Front. Syst. Neurosci. 5 (OCTOBER 2011), 1–14. doi:10.3389/fnsys.2011.00086.

Kumral, D., Şansal, F., Cesnaite, E., Mahjoory, K., Al, E., Gaebler, M., Nikulin, V.V., Villringer, A., 2020. BOLD and EEG signal variability at rest differently relate to aging in the human brain. Neuroimage 207. doi:10.1016/j.neuroimage.2019.116373.

Levy, G., 2007. The relationship of Parkinson disease with aging. Arch. Neurol. 64 (9), 1242–1246. doi:10.1001/archneur.64.9.1242.

Levy, R., Hutchison, W.D., Lozano, A.M., Dostrovsky, J.O., 2002. Synchronized neuronal discharge in the basal ganglia of Parkinsonian patients is limited to oscillatory activity. J. Neurosci. 22 (7), 2855–2861. doi:10.1523/jneurosci.22-07-02855.2002.

Little, S., Brown, P., 2014. The functional role of beta oscillations in Parkinson's disease. Parkinson. Relat. Disord. 20 (SUPPL.1), S44–S48. doi:10.1016/S1353-8020(13)70013-0.

Lofredi, R., Tan, H., Neumann, W.J., Yeh, C.H., Schneider, G.H., Kühn, A.A., Brown, P., 2019. Beta bursts during continuous movements accompany the velocity decrement in Parkinson's disease patients. Neurobiol. Dis. 127 (March), 462–471. doi:10.1016/j.nbd.2019.03.013.

López-Azcárate, J., Tainta, M., Rodríguez-Oroz, M.C., Valencia, M., González, R., Guridi, J., Iriarte, J., Obeso, J.A., Artieda, J., Alegre, M., 2010. Coupling between beta and high-frequency activity in the human subthalamic nucleus may be a pathophysiological mechanism in Parkinson's disease. J. Neurosci. 30 (19), 6667–6677. doi:10.1523/JNEUROSCI.5459-09.2010.

Louis, E.D., Bennett, D.A., 2007. Mild Parkinsonian signs: an overview of an emerging concept. Mov. Disord. 22 (12), 1681–1688. doi:10.1002/mds.21433.

Lundqvist, M., Herman, P., Lansner, A., 2011. Theta and gamma power increases and alpha/beta power decreases with memory load in an attractor network model. J. Cogn. Neurosci. 23 (10), 3008–3020. doi:10.1162/jocn_a_00029.

Lundqvist, M., Herman, P., Warden, M.R., Brincat, S.L., Miller, E.K., 2018. Gamma and beta bursts during working memory readout suggest roles in its volitional control. Nat. Commun. 9 (1), 1–12. doi:10.1038/s41467-017-02791-8.

Malekmohammadi, M., AuYong, N., Ricks-Oddie, J., Bordelon, Y., Pouratian, N., 2018. Pallidal deep brain stimulation modulates excessive cortical high β phase amplitude coupling in Parkinson disease. Brain Stimul. 11 (3), 607–617. doi:10.1016/j.brs.2018.01.028.

Manning, J.R., Jacobs, J., Fried, I., Kahana, M.J., 2009. Broadband shifts in local field potential power spectra are correlated with single-neuron spiking in humans. J. Neurosci. 29 (43), 13613–13620. doi:10.1523/JNEUROSCI.2041-09.2009.

Marsili, L., Rizzo, G., Colosimo, C., 2018. Diagnostic criteria for Parkinson's disease: from James Parkinson to the concept of prodromal disease. Front. Neurol. 9 (MAR), 1–10. doi:10.3389/fneur.2018.00156.

McAvinue, L.P., Habekost, T., Johnson, K.A., Kyllingsbæk, S., Vangkilde, S., Bundesen, C., Robertson, I.H., 2012. Sustained attention, attentional selectivity, and attentional capacity across the lifespan. Attention, Percept. Psychophys. 74 (8), 1570–1582. doi:10.3758/s13414-012-0352-6.

McFarland, N.R., Haber, S.N., 2002. Thalamic relay nuclei of the basal ganglia form both reciprocal and nonreciprocal cortical connections, linking multiple frontal cortical areas. J. Neurosci. 22 (18), 8117–8132. doi:10.1523/jneurosci.22-18-08117.2002.

Meidahl, A.C., Moll, C.K.E., van Wijk, B.C.M., Gulberti, A., Tinkhauser, G., Westphal, M., Engel, A.K., Hamel, W., Brown, P., Sharott, A., 2019. Synchronised spiking activity underlies phase amplitude coupling in the subthalamic nucleus of Parkinson's disease patients. Neurobiol. Dis. 127, 101–113. doi:10.1016/j.nbd.2019.02.005.

Melgari, J.M., Curcio, G., Mastrolilli, F., Salomone, G., Trotta, L., Tombini, M., Biase, L.Di, Scrascia, F., Fini, R., Fabrizio, E., Rossini, P.M., Vernieri, F, 2014. Alpha and beta EEG power reflects L-dopa acute administration in parkinsonian patients. Front. Aging Neurosci. 6 (OCT), 1–7. doi:10.3389/fnagi.2014.00302.

Michelmann, S., Bowman, H., Hanslmayr, S., 2016. The temporal signature of memories: identification of a general mechanism for dynamic memory replay in humans. PLoS Biol. 14 (8), 1–27. doi:10.1371/journal.pbio.1002528.

Michely, J., Volz, L.J., Hoffstaedter, F., Tittgemeyer, M., Eickhoff, S.B., Fink, G.R., Grefkes, C., 2018. Network connectivity of motor control in the ageing brain. NeuroImage: Clin. 18 (February), 443–455. doi:10.1016/j.nicl.2018.02.001.

Miller, A.M., Miocinovic, S., Swann, N.C., Rajagopalan, S.S., Darevsky, D.M., Gilron, R., de Hemptinne, C., Ostrem, J.L., Starr, P.A., 2019. Effect of levodopa on electroencephalographic biomarkers of the parkinsonian state. J. Neurophysiol. 122 (1), 290–299. doi:10.1152/jn.00141.2019.

Miller, K.J., Sorensen, L.B., Ojemann, J.G., Den Nijs, M., 2009. Power-law scaling in the brain surface electric potential. PLoS Comput. Biol. 5 (12). doi:10.1371/journal.pcbi.1000609.

Müller, E.J., Robinson, P.A., 2018. Suppression of parkinsonian beta oscillations by deep brain stimulation: determination of effective protocols. Front. Comput. Neurosci. 12 (December), 1–16. doi:10.3389/fncom.2018.00098.

Murthy, V.N., Fetz, E.E., 1992. Coherent 25- To 35-Hz oscillations in the sensorimotor cortex of awake behaving monkeys. PNAS 89 (12), 5670–5674. doi:10.1073/pnas.89.12.5670.

Nomi, J.S., Bolt, T.S., Chiemeka Ezie, C.E., Uddin, L.Q., Heller, A.S., 2017. Moment-to-moment BOLD signal variability reflects regional changes in neural flexibility across the lifespan. J. Neurosci. 37 (22), 5539–5548. doi:10.1523/JNEUROSCI.3408-16.2017.

O'Keeffe, A.B., Malekmohammadi, M., Sparks, H., Pouratian, N., 2020. Synchrony drives motor cortex beta bursting,waveform dynamics, and phase-amplitude cou-

pling in parkinson's disease. J. Neurosci. 40 (30), 5833–5846. doi:10.1523/JNEUROSCI.1996-19.2020.

Oostenveld, R., Fries, P., Maris, E., Schoffelen, J.M., 2011. FieldTrip: open source software for advanced analysis of MEG, EEG, and invasive electrophysiological data. Comput. Intell. Neurosci. 2011. doi:10.1155/2011/156869.

Oswal, A., Beudel, M., Zrinzo, L., Limousin, P., Hariz, M., Foltynie, T., Litvak, V., Brown, P., 2016. Deep brain stimulation modulates synchrony within spatially and spectrally distinct resting state networks in Parkinson's disease. Brain 139 (5), 1482–1496. doi:10.1093/brain/aww048.

Oswal, A., Brown, P., Litvak, V., 2013. Synchronized neural oscillations and the pathophysiology of Parkinson's disease. Curr. Opin. Neurol. 26 (6), 662–670. doi:10.1097/WCO.0000000000000034.

Pang, S.Y.Y., Ho, P.W.L., Liu, H.F., Leung, C.T., Li, L., Chang, E.E.S., Ramsden, D.B., Ho, S.L., 2019. The interplay of aging, genetics and environmental factors in the pathogenesis of Parkinson's disease. Transl. Neurodegener. 8 (1), 1–11. doi:10.1186/s40035-019-0165-9.

Pfurtscheller, G., Stancák, A., Neuper, C., 1996. Post-movement beta synchronization. A correlate of an idling motor area? Electroencephalogr. Clin. Neurophysiol. 98 (4), 281–293. doi:10.1016/0013-4694(95)00258-8.

Pollok, B., Latz, D., Krause, V., Butz, M., Schnitzler, A., 2014. Changes of motor-cortical oscillations associated with motor learning. Neuroscience 275, 47–53. doi:10.1016/j.neuroscience.2014.06.008.

Ray, N.J., Jenkinson, N., Wang, S., Holland, P., Brittain, J.S., Joint, C., Stein, J.F., Aziz, T., 2008. Local field potential beta activity in the subthalamic nucleus of patients with Parkinson's disease is associated with improvements in bradykinesia after dopamine and deep brain stimulation. Exp. Neurol. 213 (1), 108–113. doi:10.1016/j.expneurol.2008.05.008.

Reeve, A., Simcox, E., Turnbull, D., 2014. Ageing and Parkinson's disease: why is advancing age the biggest risk factor? Ageing Res. Rev. 14 (1), 19–30. doi:10.1016/j.arr.2014.01.004.

Romanella, S.M., Roe, D., Paciorek, R., Cappon, D., Ruffini, G., Menardi, A., Rossi, A., Rossi, S., Santarnecchi, E., 2020. Sleep, noninvasive brain stimulation, and the aging brain: challenges and opportunities. Ageing Res. Rev. 61. doi:10.1016/j.arr.2020.101067, (August 2019).

Rossiter, H.E., Davis, E.M., Clark, E.V., Boudrias, M.H., Ward, N.S., 2014. Beta oscillations reflect changes in motor cortex inhibition in healthy ageing. Neuroimage 91, 360–365. doi:10.1016/j.neuroimage.2014.01.012.

Rowe, J.B., Siebner, H., Filipovic, S.R., Cordivari, C., Gerschlager, W., Rothwell, J., Frackowiak, R., 2006. Aging is associated with contrasting changes in local and distant cortical connectivity in the human motor system. Neuroimage 32 (2), 747–760. doi:10.1016/j.neuroimage.2006.03.061.

Rudow, G., O'Brien, R., Savonenko, A.V., Resnick, S.M., Zonderman, A.B., Pletnikova, O., Marsh, L., Dawson, T.M., Crain, B.J., West, M.J., Troncoso, J.C., 2008. Morphometry of the human substantia nigra in ageing and Parkinson's disease. Acta Neuropathol. (Berl) 115 (4), 461–470. doi:10.1007/s00401-008-0352-8.

Sherman, M.A., Lee, S., Law, R., Haegens, S., Thorn, C.A., Hämäläinen, M.S., Moore, C.I., Jones, S.R., 2016. Neural mechanisms of transient neocortical beta rhythms: converging evidence from humans, computational modeling, monkeys, and mice. PNAS 113 (33), E4885–E4894. doi:10.1073/pnas.1604135113.

Shi, J., Liu, J., Qu, Q., 2014. Handedness and dominant side of symptoms in Parkinson's disease. Med. Clin. (Barc) 142 (4), 141–144. doi:10.1016/j.medcli.2012.11.028.

Sibille, E., 2013. Molecular aging of the brain, neuroplasticity, and vulnerability to depression and other brain-related disorders. Dialogues Clin. Neurosci. 15 (1), 53–65.

Stoffers, D., Bosboom, J.L.W., Deijen, J.B., Wolters, E.C., Berendse, H.W., Stam, C.J., 2007. Slowing of oscillatory brain activity is a stable characteristic of Parkinson's disease without dementia. Brain 130 (7), 1847–1860. doi:10.1093/brain/awm034.

Swann, N.C., De Hemptinne, C., Aron, A.R., Ostrem, J.L., Knight, R.T., Starr, P.A., 2015. Elevated synchrony in Parkinson disease detected with electroencephalography. Ann. Neurol. 78 (5), 742–750. doi:10.1002/ana.24507.

Tinkhauser, G., Pogosyan, A., Little, S., Beudel, M., Herz, D.M., Tan, H., Brown, P., 2017a. The modulatory effect of adaptive deep brain stimulation on beta bursts in Parkinson's disease. Brain 140 (4), 1053–1067. doi:10.1093/brain/awx010.

Tinkhauser, G., Pogosyan, A., Tan, H., Herz, D.M., Kühn, A.A., Brown, P., 2017b. Beta burst dynamics in Parkinson's disease off and on dopaminergic medication. Brain 140 (11), 2968–2981. doi:10.1093/brain/awx252.

Tinkhauser, G., Torrecillos, F., Duclos, Y., Tan, H., Pogosyan, A., Fischer, P., Carron, R., Welter, M.L., Karachi, C., Vandenberghe, W., Nuttin, B., Witjas, T., Régis, J., Azulay, J.P., Eusebio, A., Brown, P., 2018. Beta burst coupling across the motor circuit in Parkinson's disease. Neurobiol. Dis. 117 (June), 217–225. doi:10.1016/j.nbd.2018.06.007.

Tort, A.B.L., Kramer, M.A., Thorn, C., Gibson, D.J., Kubota, Y., Graybiel, A.M., Kopell, N.J., 2008. Dynamic cross-frequency couplings of local field potential oscillations in rat striatum and hippocampus during performance of a T-maze task. PNAS 105 (51), 20517–20522. doi:10.1073/pnas.0810524105.

van Wijk, B.C.M., Beudel, M., Jha, A., Oswal, A., Foltynie, T., Hariz, M.I., Limousin, P., Zrinzo, L., Aziz, T.Z., Green, A.L., Brown, P., Litvak, V., 2016. Subthalamic nucleus phase-amplitude coupling correlates with motor impairment in Parkinson's disease. Clin. Neurophysiol. 127 (4), 2010–2019. doi:10.1016/j.clinph.2016.01.015.

Ward, N.S., Frackowiak, R.S.J., 2003. Age-related changes in the neural correlates of motor performance. Brain 126 (4), 873–888. doi:10.1093/brain/awg071.

Weinberger, M., Mahant, N., Hutchison, W.D., Lozano, A.M., Moro, E., Hodaie, M., Lang, A.E., Dostrovsky, J.O., 2006. Beta oscillatory activity in the subthalamic nucleus and its relation to dopaminergic response in Parkinson's disease. J. Neurophysiol. 96 (6), 3248–3256. doi:10.1152/jn.00697.2006.

Wessel, J.R., Aron, A.R., 2017. On the globality of motor suppression: unexpected events and their influence on behavior and cognition. Neuron 93 (2), 259–280. doi:10.1016/j.neuron.2016.12.013.

Whitmer, D., de Solages, C., Hill, B., Yu, H., Henderson, J.M., Bronte-Stewart, H., 2012. High frequency deep brain stimulation attenuates subthalamic and cortical rhythms in Parkinson's disease. Front. Hum. Neurosci. 6 (JUNE 2012), 1–18. doi:10.3389/fnhum.2012.00155.

Wingeier, B., Tcheng, T., Koop, M.M., Hill, B.C., Heit, G., Bronte-Stewart, H.M., 2006. Intra-operative STN DBS attenuates the prominent beta rhythm in the STN in Parkinson's disease. Exp. Neurol. 197 (1), 244–251. doi:10.1016/j.expneurol.2005.09.016.

Yau, Y., Zeighami, Y., Baker, T.E., Larcher, K., Vainik, U., Dadar, M., Fonov, V.S., Hagmann, P., Griffa, A., Mišić, B., Collins, D.L., Dagher, A., 2018. Network connectivity determines cortical thinning in early Parkinson's disease progression. Nat. Commun. 9 (1), 1–10. doi:10.1038/s41467-017-02416-0.

Benjamini, Yoav, Hochberg, Yosef, 1995. Controlling the false discovery rate: a practical and powerful approach to multiple testing. J. R. Stat. Soc. Ser. B (Methodol.) 57 (1), 289–300.

Zappasodi, F., Marzetti, L., Olejarczyk, E., Tecchio, F., Pizzella, V., 2015. Age-related changes in electroencephalographic signal complexity. PLoS ONE 10 (11), 1–13. doi:10.1371/journal.pone.0141995.

Zeighami, Y., Fereshtehnejad, S.M., Dadar, M., Collins, D.L., Postuma, R.B., Mišić, B., Dagher, A., 2019. A clinical-anatomical signature of Parkinson's disease identified with partial least squares and magnetic resonance imaging. Neuroimage 190 (December), 69–78. doi:10.1016/j.neuroimage.2017.12.050.

Zhuang, F.J., Chen, Y., He, W.B., Cai, Z.Y., 2018. Prevalence of white matter hyperintensities increases with age. Neural Regen. Res. 13 (12), 2141–2146. doi:10.4103/1673-5374.241465.